



# Assessment of potentially toxic heavy elements and $^{137}\text{Cs}$ in the Polesie State Radiation and Ecological Reserve, Belarus

Nikita Yushin<sup>1</sup> · Mohamed M. Ghoneim<sup>1,2,3</sup> · Aleksander Nikitin<sup>4</sup> · Egor Mischenko<sup>4</sup> · Diana Suhareva<sup>4</sup> · Olga Shurankova<sup>4</sup> · Galina Leferd<sup>4</sup> · Aliaksandr Sudnik<sup>5</sup> · Evgeny Shavalda<sup>5</sup> · Inga Zinicovscaia<sup>1,6</sup>

Received: 17 March 2025 / Accepted: 28 July 2025  
© Akadémiai Kiadó Zrt 2025

## Abstract

Soil pollution by potentially toxic elements (PTEs) and radionuclides, such as  $^{137}\text{Cs}$ , poses environmental and health risks, particularly in areas affected by nuclear accidents. This study evaluates PTE and  $^{137}\text{Cs}$  concentrations in soil from the Polesie State Radiation and Ecological Reserve in Belarus, a region impacted by the 1986 Chernobyl disaster. Soil samples (0–5 cm and 5–20 cm depths) were analyzed using ICP-OES, a direct mercury analyzer, and gamma spectrometry. While PTE levels were below background thresholds,  $^{137}\text{Cs}$  activity in topsoil (up to 117,947 Bq/kg) far exceeded global averages, underscoring the enduring legacy of Chernobyl contamination and the need for continued monitoring and remediation efforts.

**Keywords** Potentially toxic elements<sup>137</sup>Cs · ICP-OES · Belarus · Low-background gamma spectrometry · PTEs

## Introduction

Pollution from potentially toxic elements (PTEs) represents a pressing global environmental challenge, with profound implications for soil health, agricultural productivity, and the well-being of ecosystems, humans, and wildlife. PTEs, including lead (Pb), zinc (Zn), cadmium (Cd), mercury (Hg), chromium (Cr), and nickel (Ni), are characterized by their environmental persistence, bioaccumulation potential, and toxicological effects, which range from acute toxicity to

carcinogenicity. The prolonged presence of PTEs in ecosystems can result in ecological degradation, soil contamination, and reduced agricultural yields, threatening food security and biodiversity. Chronic exposure to these elements, particularly through bioaccumulation and biomagnification in food chains, poses significant health risks. For instance, lead exposure is associated with neurological damage, whereas cadmium is linked to severe conditions such as kidney dysfunction and lung cancer. Mercury, particularly in its organic form as methylmercury, is highly neurotoxic, causing developmental and cognitive impairments, especially in vulnerable populations. Hexavalent chromium (Cr (VI)) is a well-known carcinogen that is primarily associated with lung cancer and respiratory disorders, whereas nickel exposure, often in occupational settings, is associated with lung and nasal cancers, dermatitis, and respiratory complications. Although zinc is an essential micronutrient, excessive exposure can lead to gastrointestinal distress, immune suppression, and metabolic imbalances. Collectively, the widespread contamination and toxic effects of PTEs underscore the urgent need for comprehensive research, monitoring, and remediation strategies to mitigate their environmental and public health impacts [1–9].

The sources of PTEs can be categorized into natural (geogenic) and anthropogenic. Natural factors, such as volcanic eruptions and weathering, contribute to background levels, while human activities industrial processes, wastewater

✉ Mohamed M. Ghoneim  
moh.gho@mail.ru

- <sup>1</sup> Joint Institute for Nuclear Research, 6 Joliot-Curie Str., Dubna, Moscow Region 141980, Russia
- <sup>2</sup> Nuclear Materials Authority of Egypt, Maadi, P.O. Box 530, Cairo 11381, Egypt
- <sup>3</sup> Academy of Scientific Research and Technology (ASRT), Cairo, Egypt
- <sup>4</sup> Institute of Radiobiology of the National Academy of Sciences of Belarus, Fedjuninskogo Str, 4, 246007 Gomel, Belarus
- <sup>5</sup> V.F. Kuprevich Institute of Experimental Botany of the National Academy of Sciences of Belarus, Akademicheskaya Str, 27, 220072 Minsk, Belarus
- <sup>6</sup> Horia Hulubei National Institute for Physics and Nuclear Engineering (IFIN-HH), Bucharest, Romania

discharge, mining, and pesticide application, substantially elevate the toxic element concentrations in soils. These anthropogenic influences have become significant drivers of PTEs pollution, exacerbating their ecological and health risks [10–13].

In addition to PTEs, radionuclides like cesium-137 ( $^{137}\text{Cs}$ ) are important contaminants resulting from nuclear activities.  $^{137}\text{Cs}$ , primarily generated through fission processes, has been particularly pervasive due to historical nuclear weapons testing and significant accidents such as the 1986 Chernobyl disaster, which dispersed substantial amounts of this radionuclide across vast areas, particularly affecting Belarus, Ukraine, and Russia. The extended half-life of  $^{137}\text{Cs}$  (approximately 30 years) contributes to its long-term presence in soil and ecosystems, necessitating continued monitoring and management [14–18].

The Chernobyl accident (April 26, 1986) resulted in the contamination of a large area of Europe with man-made radionuclides. The most contaminated part of the Republic of Belarus (the Byelorussian SSR at the time of the accident) was defined as an evacuation (exclusion) zone, where the Polesie State Radiation and Ecological Reserve (PSRER) was later formed. Currently, this territory is characterized by high  $^{137}\text{Cs}$  contamination, along with long-lived isotopes of transuranic elements ( $^{238,239,240,241}\text{Pu}$ ,  $^{241}\text{Am}$ ) and  $^{90}\text{Sr}$ . The contamination is mosaic and uneven, both across the entire territory and within individual areas. Therefore, the  $^{137}\text{Cs}$  contamination levels can vary by 1.5–10 times within one forest compartment. Moreover, the higher the average pollution density of an area, the stronger its mosaic nature [19]. The mosaic nature of the contamination was caused by both the nature of the initial fallout of the radionuclides, which was strongly influenced by the terrain and vegetation, and the subsequent horizontal redistribution of the radionuclides. In areas close to the Chernobyl nuclear power plant, fuel particles with varying degrees of dispersion make a significant contribution to the level of contamination, its spatial heterogeneity, and biological availability of radionuclides [19].

According to large-scale surveys conducted in 2019–2022 by the Institute of Radiobiology of the National Academy of Sciences of Belarus, the level of soil contamination with  $^{137}\text{Cs}$  is in the range of 174–5616 kBq/m<sup>2</sup> with a specific activity of the radionuclide in the upper 20-cm soil layer ranging from 0.75 to 71.28 KBq/kg. The highest levels of contamination are characterized for the southeastern part of the PGRERZ, in the area of the former settlements of Kryuki, Zhelibor, Mikhalevka, and Kulazhin [20, 21].

This study aims to assess the levels of PTEs and  $^{137}\text{Cs}$  in soil samples from the Polesie State Radiation and Ecological Reserve, examining the contamination levels, enrichment indices, geo-accumulation indices, and potential ecological risks. The primary objectives are to quantify

the concentrations of PTEs and  $^{137}\text{Cs}$  and to evaluate the associated risks to ecosystem health and human safety. Understanding these complex ecological processes in contaminated environments is crucial for developing effective strategies for environmental management, risk mitigation, and sustainable development within the reserve.

## Materials and methods

### Sampling

From August to October 2023, soil samples were collected from the Polesie State Radiation and Ecological Reserve at depths of 0–5 cm and 5–20 cm across the entire study area (Fig. 1). The sampling procedure adhered to the Russian standard GOST 17.4.4.02-84 [22]. A total of 45 soil samples were collected: 18 samples at 0–5 cm and 27 samples at 5–20 cm]. Following collection, extraneous materials such as leaves, grass, plant roots, and pebbles were removed from the samples. The remaining soil material was homogenized and dried at 105 °C. Each soil replicate was individually prepared and analyzed to ensure accuracy and consistency in the results.

### Elemental analysis

The content of 11 elements, Cu, Cd, Co, Pb, Zn, V, Cr, Ni, Mn, P, and Fe, in the analyzed soil samples, was determined using an ICP-OES PlasmaQuant PQ 9000 Elite spectrometer (Analytik Jena, Jena, Germany). Before analysis, the soil samples were digested using the MARS6 system. Detailed methodologies for sample preparation have been described in previous studies [23, 24].

The mercury content was measured using a direct mercury analyzer (DMA-80 evo), which does not require specialized sample preparation. To ensure the accuracy and reliability of the results, standard reference materials (IAEA-458 and NIST-2709a) were used for quality control. Additional details regarding the quality control procedures are provided in Table 1.

The measurement of  $^{137}\text{Cs}$  activity levels in the soil samples was ensured by a gamma-radiometer RKG-AT1320A equipped with a NaI (TI)  $\phi 63 \times 63$  mm scintillation detector. (Atomtex, Belarus). The counting efficiency was calibrated in accordance with the procedure specified in the equipment manual using standard gamma source  $^{40}\text{K}$ , which is supplied by the manufacturer as part of the device package. The reliability of the measurements was validated using a reference source SOKK-951/12–22 (Belarusian State Institute of Metrology, Belarus) with a  $^{137}\text{Cs}$  activity of  $2897 \pm 320$  Bq/kg ( $k=2$ ). The soil samples were measured in counting

**Fig. 1** Map of soil sampling in the Radiation and Ecological Reserve of Polesie State, Belarus

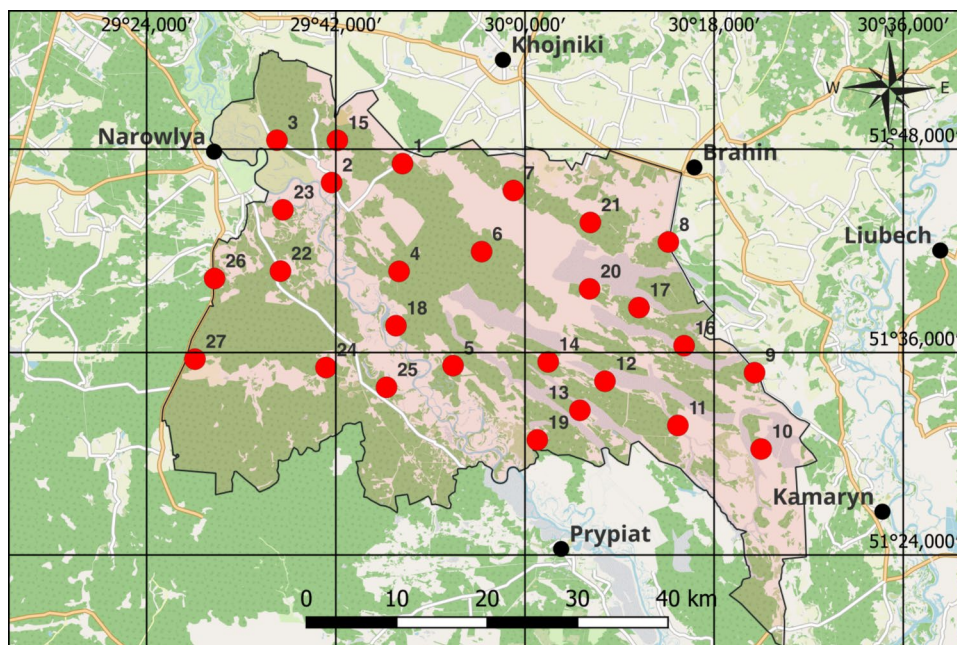


**Table 1** Quality control of ICP-OES measurements

Element	2709a				458			
	Experimental value (mg/kg)	SD	Passport value	Recovery, %	Experimental value (mg/kg)	SD	Passport value	Recovery, %
Cu	34.2	0.39	33.9	101	45.7	0.4	48.1	95
Cd	0.4	0.01	0.371	108	0.5	0	0.49	99
Co	13.4	0.05	12.8	105	14.7	0.1	15.6	94
Pb	16.7	0.17	17.3	96	36.4	0.5	35.5	103
Zn	100	0.14	103	97	159	0.6	154	103
V	110	0.31	110	100	97.8	0.5	99.8	98
Cr	116	0.41	130	90	95.3	0.6	91.5	104
Ni	75.8	0.48	85	89	39.1	0.2	40	98
Mn	545	4.93	529	103	904	5.7	886	102
P	722	8.1	688	105	723	5.4	–	–
Fe	35,030	84.3	33,600	104	39,790	251	40,700	98

vessels with a cylindrical geometry of  $\phi 63 \times 35$  mm. Each spectrum was acquired with a live time of 900 s.

Owing to the relatively high activity of  $^{137}\text{Cs}$  in the soil samples, the photopeak at 662 keV is clearly distinguishable in the gamma spectrum, ensuring high reliability in both the identification and quantification of the radionuclide (Fig. 2).

### Assessment of pollution using environmental pollution indices

The PTE contamination in the studied soil samples was assessed by applying ecological risk assessment approaches such as the Geo-accumulation Index ( $I_{\text{geo}}$ ), Contamination Factor (CF), Pollution Load Index (PLI), Enrichment Factor

(EF), Single-Element Pollution Index (SEPI), and Multi-Element Pollution Index (MEPI).

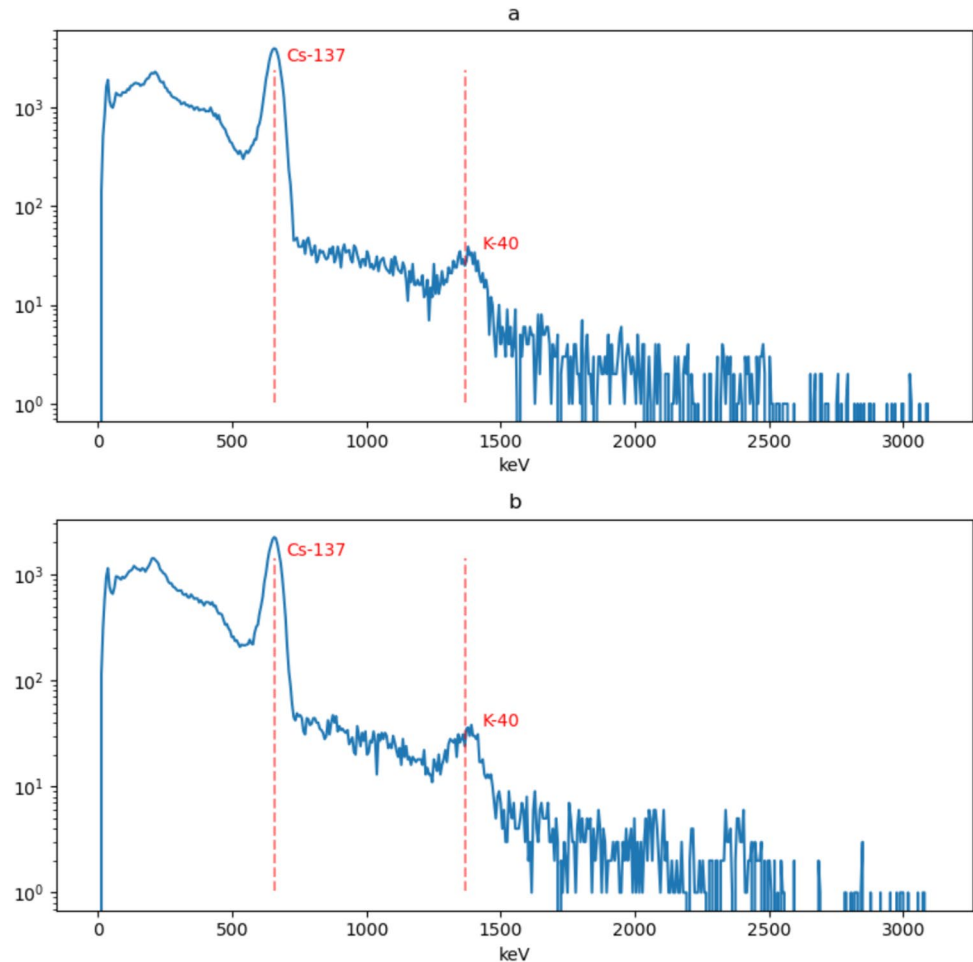
### Geo-accumulation index ( $I_{\text{geo}}$ )

The Geo-accumulation Index ( $I_{\text{geo}}$ ) serves as a critical tool for assessing soil contamination by comparing the metal concentrations to the natural background levels. The formula

$$I_{\text{geo}} = \log_2 \left( \frac{C_{\text{soil}}}{1.5B_{\text{soil}}} \right) \quad (1)$$

allows researchers to quantify the degree of anthropogenic influence on the soil metal content, where  $C_{\text{soil}}$  represents

**Fig. 2** Gamma-ray spectra recorded with the RKG-AT1320A gamma-radiometer for soil samples containing  $^{137}\text{Cs}$  at activity concentrations of  $9145 \pm 549 \text{ Bq/kg}$  (a) and  $5223 \pm 312 \text{ Bq/kg}$  (b)



the metal concentration in the soil and  $B_{\text{soil}}$  represents the background concentration of the metal. The interpretation of the  $I_{\text{geo}}$  values is as follows:  $I_{\text{geo}}$  values less than 0 indicate that the soil is uncontaminated; values between 0 and 1 suggest moderate contamination; values between 1 and 2 imply moderate to strong contamination; values between 2 and 3 denote strong contamination; and values greater than 3 signify extremely contaminated soil [25–28].

### Contamination factor (CF)

The content of metals in soil is evaluated by comparing it to a reference value, such as the average abundance found in the Earth's crust. CF is used to assess the level of soil pollution using the formula:

$$CF = \frac{C_{\text{soil}}}{C_{\text{ref}}} \quad (2)$$

where  $C_{\text{soil}}$  represents the content of the metal in the soil, and  $C_{\text{ref}}$  denotes the reference value. The reference value of [29] was selected. Contamination levels are then classified

based on their intensity using a scale from 0 to 6: a score of 0 indicates no contamination; 1 signifies low to medium levels of contamination; 2 represents moderate contamination; 3 indicates moderate to strong contamination; 4 reflects strong pollution; 5 denotes strong to very strong pollution; and 6 indicates very high levels of contamination [29, 30].

### Pollution load index (PLI)

The pollution load index (PLI) assesses the overall pollution status of soils contaminated by multiple heavy metals. The contamination factor for each metal was calculated as the ratio of the concentration of the metal in the soil to its background or reference value [29, 31]. The formula is:

$$PLI = \sqrt[n]{CF_1 * CF_2 \dots CF_n} \quad (3)$$

$CF_n$  represent the contamination factors of individual metals. PLI values less than 1 indicate unpolluted soil; values between 1 and 2 suggest moderately polluted soil; values between 2 and 5 denote heavily polluted soil; and values greater than 5 indicate severe pollution [32].

## Enrichment factor (EF)

The metal concentration in the soil was compared to a conservative element (e.g. Fe). The formula for calculating the EF is:

$$EF = \frac{C_{\text{soil}}}{C_{\text{ref}}} \cdot \frac{B_{\text{ref}}}{B_{\text{soil}}} \quad (4)$$

where  $C_{\text{soil}}$  represents the metal concentration in the soil,  $B_{\text{soil}}$  represents the background metal concentration,  $C_{\text{ref}}$  represents the concentration of the conservative soil element, and  $B_{\text{ref}}$  represents the background concentration of the conservative element. This comparison helps to identify whether the metal concentrations are influenced by anthropogenic activities or if they are within natural variability. EF values less than 1 indicate no enrichment; values between 1 and 3 suggest minor enrichment; values between 3 and 5 denote moderate enrichment; values between 5 and 10 reflect significant enrichment; and values greater than 10 indicate very high enrichment [32–34].

## Potential single-element pollution index (SEPI)

The potential toxicity of PTEs can be assessed by evaluating their content and calculating their corresponding toxic units. This approach, as proposed by [31], provides a systematic framework for quantifying the ecological risk posed by heavy metals in environmental systems. By comparing the measured concentrations of heavy metals to established toxicity thresholds, researchers can determine the extent of contamination and its potential impact on ecosystems and human health using the following formula:

$$SEPI = \frac{C_{\text{soil}}}{C_{\text{ref}} \cdot T_{\text{unit}}} \quad (5)$$

where  $C_{\text{soil}}$  represents the metal concentration in the soil,  $C_{\text{ref}}$  represents the reference value, and  $T_{\text{unit}}$  represents the toxic response factor assigned to each metal, e.g., Cr: 2, Cu: 5, Cd: 30, Zn: 1, Pb: 5 [31, 35]. The overall Multi-Element Pollution Index (MEPI) or Ecological Risk Index (RI) is the sum of the potential ecological risk index of each elements.

$$MEPI = \frac{1}{n} \sum_{i=1}^n SEPI_i \quad (6)$$

where  $n$  is the count of elements. It can be categorized into RI values less than 150, indicating low ecological risk; values between 150 and 300, indicating moderate ecological risk; and values between 300 and 600, indicating high ecological risk [31].

## Results and discussion

### Basic statistics

The analysis of soil samples from the study area revealed the mean content of elements in the following descending order: Fe > P > Mn > Zn > Pb > Co > Cr > V > Ni > Cu > Cd > Hg. This ranking indicates the relative abundance of these elements in the soil, with iron (Fe) being the most dominant and mercury (Hg) the least. A comparison of the average concentrations of elements in the topsoil (0–5 cm) and lower soil (5–20 cm) with the background levels provided by [29] was conducted to assess the enrichment and potential pollution (Table 2). The results showed that the content of Ni in the top soil (5.9 mg/kg) was slightly above the background level. All other elements, including Cu, Cd, Co, Pb, Zn, V, Cr, Mn, Fe, and Hg, exhibited content significantly lower than the background levels in both the topsoil and lower soil layers. This suggests minimal contamination from these elements in the study area.

**Table 2** Basic statistics of PTEs and background values (in mg/kg) for soil samples collected from the Radiation and Ecological Reserve of Polesie State, Belarus

Elements	0–5 cm				5–20 cm				Background [29]
	Mean	Min–Max	Med	Stdev	Mean	Min–max	Med	Stdev	
Cu	2.4	1.2–5.4	11.4	1.1	0.88	0.54–1.6	0.9	0.2	11.4
Cd	0.1	0–0.2	1.8	0	0.08	0.05–0.1	0.1	0.01	1.8
Co	4.5	3.4–5.3	33.5	0.5	5.76	4.3–6.8	5.8	0.6	33.5
Pb	9.3	4.9–27.5	15.6	5	4.61	2.85–6.5	4.4	0.9	15.6
Zn	13.1	4.5–27.5	48.4	7.8	6.74	2.9–42.2	5.1	7.11	48.4
V	6.1	2.8–15.6	10.9	3	3.24	1.8–5.1	3	0.9	10.9
Cr	6.9	2.8–14.2	30.3	2.8	3.2	1.71–5.5	2.8	1.2	30.3
Ni	6	1.4–10.7	3.6	2.8	2.9	0.79–7.1	2	1.8	3.6
Mn	147.3	15.9–465	703	137	73.8	13.2–216	66	49.9	703
P	269	110–542	ND	110	198	98.9–377	198	49.8	ND
Fe	2241	957–5245	8403	1159	1323	595–2191	1219	461	8403
Hg	0.05	0.01–0.22	1.3	0.05	0.02	0.003–0.05	0.01	0.01	1.3

The concentration of most elements was higher in the topsoil than in the lower soil, indicating surface deposition of contaminants. For instance, Ni exhibited a higher concentration in the topsoil (5.9 mg/kg) compared with the lower soil (2.9 mg/kg). The deeper soil layer (5–20 cm) generally demonstrates lower average metal content relative to the surface layer, potentially due to processes such as leaching, dilution over time, or reduced anthropogenic influence with depth [36]. However, an exception was observed for Co, which was slightly higher in the lower soil (5.7 mg/kg) than in the topsoil (4.5 mg/kg). This exception suggests a predominance of geogenic origins for this PTE [36, 37].

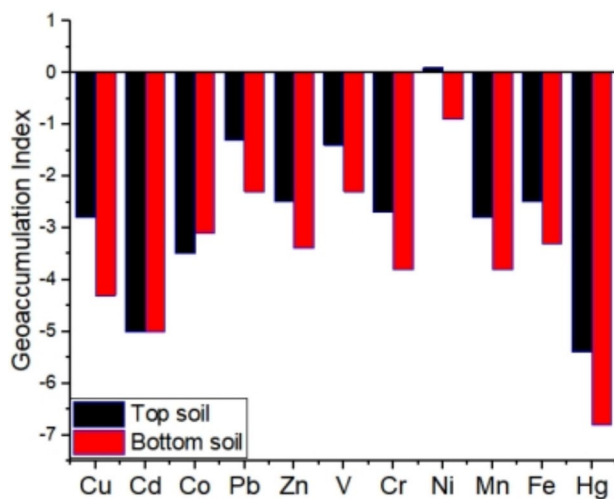


**Fig. 3** The Geo-accumulation index of the soil samples collected from the Radiation and Ecological Reserve of Polesie State, Belarus

### Geoaccumulation index ( $I_{geo}$ )

The geoaccumulation index ( $I_{geo}$ ) analysis indicates that the soil in the study area remains consistently below the natural background levels and is classified as uncontaminated for all PTEs at both examined depths (0–5 cm and 5–20 cm) (Fig. 3). A minor increase in nickel (Ni) levels is observed at the 0–5 cm depth; however, it does not pose a significant risk. Nonetheless, long-term monitoring is recommended to ensure soil health.

### Contamination factors (CF)

The contamination factor for most PTEs was notably higher in the 0–5 cm depth compared to the 5–20 cm depth, with the standard deviation in the 0–5 cm layer generally higher than in the 5–20 cm layer. This indicates a more variable contamination level in the topsoil. Despite this variability, the concentrations of all PTEs were well below their respective background levels, confirming minimal contamination. The contamination levels were consistent across both depths (0–5 cm and 5–20 cm). Ni exhibited the highest CF values (1.6 at 0–5 cm and 0.8 at 5–20 cm), but these values still fall under the low contamination category (Table 3).

### Pollution load index (PLI)

The Pollution Load Index (PLI) was used to assess the overall contamination status of the soils at two depths (0–5 cm and 5–20 cm) in the study area. In the surface layer (0–5 cm), the PLI values ranged from 0.09 (min) to 0.40 (max), with an average of 0.23 and a median of 0.2, indicating low levels of pollution. Similarly, in the deeper layer (5–20 cm), the PLI values were lower, ranging from 0.07 (min) to 0.17 (max), with an average of 0.13 and a median of 0.11, further confirming minimal pollution. The standard deviation (step)

**Table 3** Contamination factors (CF) and Pollution Load Index (PLI) for major and trace elements (potentially toxic metals) in soil samples from the study area at two depths (0–5 cm and 5–20 cm)

	Element	0–5 cm				5–20 cm			
		Mean	Min–max	Med	Stdev	Mean	Min–max	Med	Stdev
Contamination factors (CT)	Cu	0.21	0.1–0.4	0.2	0.09	0.08	0.05–0.14	0.08	0.02
	Cd	0.05	0.02–0.09	0.04	0.02	0.05	0.03–0.06	0.05	0.01
	Co	0.13	0.1–0.16	0.13	0.02	0.17	0.13–0.2	0.17	0.02
	Pb	0.59	0.3–1.7	0.55	0.32	0.3	0.18–0.42	0.28	0.06
	Zn	0.27	0.09–0.5	0.2	0.16	0.14	0.06–0.87	0.11	0.15
	V	0.56	0.2–1.4	0.47	0.28	0.3	0.16–0.47	0.27	0.09
	Cr	0.23	0.09–0.47	0.22	0.09	0.11	0.06–0.18	0.09	0.04
	Ni	1.66	0.38–2.9	1.71	0.79	0.81	0.22–1.97	0.56	0.51
	Mn	0.21	0.02–0.6	0.13	0.19	0.1	0.02–0.31	0.09	0.07
	Fe	0.27	0.11–0.62	0.26	0.14	0.16	0.07–0.26	0.15	0.05
	Hg	0.04	0.01–0.1	0.02	0.04	0.01	0.01–0.4	0.01	0.01
Pollution load index	PLI	0.2	0.09–0.4	0.2	0.09	0.1	0.07–0.17	0.11	0.03

of 0.09 for the 0–5 cm layer and 0.03 for the 5–20 cm layer suggests relatively consistent and low variability in pollution levels across both depths (Table 3). Overall, the PLI values for both soil layers are well below the threshold of 1, indicating that the soils are uncontaminated and pose no significant environmental risk. These findings align with the enrichment factor (EF) and geoaccumulation index ( $I_{geo}$ ) analyses, reinforcing the conclusion that the study area remains largely unaffected by heavy metal pollution.

### Enrichment factor

Soil layer analysis using enrichment factors (EFs) provides valuable insights into the distribution of potentially toxic elements (PTEs) and the potential anthropogenic impacts on soil quality. In the uppermost soil layer, EFs revealed a range of values indicative of varying levels of contamination. Cd showed an EF as low as 0.18, indicating depletion or minimal enrichment, while Ni had an EF of 6.21, suggesting significant enrichment. Pb and V displayed moderate enrichment with EFs of 2.22 and 2.08, respectively. Elements like (Cu, Co, Zn, Cr, Mn, and Hg) were found near or below the background concentrations. The high standard deviation for Ni (stdev = 3.68) and Zn (stdev = 0.49) indicates spatial nonuniformity in their distribution across this layer. In contrast to the upper stratum, the deeper soil layer generally exhibited lower average EFs: Cd's EF was approximately 0.30; Ni's was about 5.12; Pb showed a moderate enrichment with an EF around 0.87; V's enrichment was also moderate (EF 1.8). Similar to the upper layer, Cu, Co, Zn, Cr, Mn, and Hg remained close to the background levels. Again, notable was the significant variability in Ni (stdev = 4.3), and Zn (stdev = 1.5), reflecting the heterogeneous distributions within this deeper stratum. The histogram shows a comparison between the enrichment factors of various PTEs in the top and bottom layers of the study area (Fig. 4).

### Ecological risk indices (RI)

The ecological risk indices (RI) analysis indicates low ecological risk in the 0–5 cm soil depth, with average, minimum, and median RI values all significantly below 150. A maximum RI of 32.3 suggests localized hotspots with slightly elevated risks, primarily driven by Ni (average RI of 8.28) and Pb (average RI of 2.9). At the 5–20 cm depth, the average RI was 9.31, with a minimum of 5.3 and a median of 8.1, reinforcing the low-risk conclusion as all values remained below 150. (Table 4).

### Correlation analysis

The Pearson correlation analysis for soil samples from the Polesie State Radiation and Ecological Reserve in Belarus

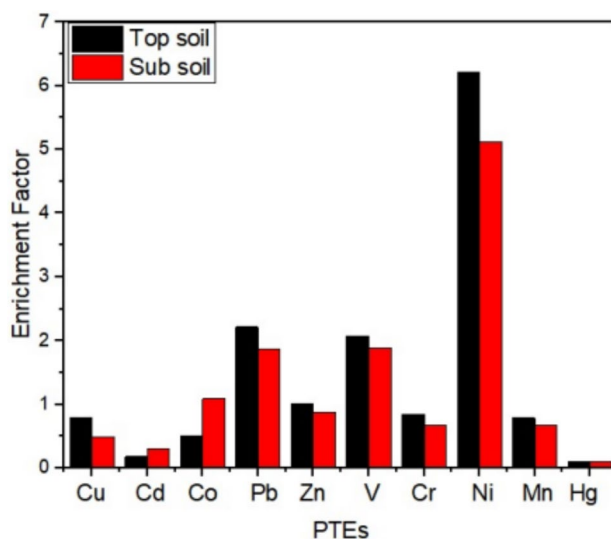


Fig. 4 Enrichment factor of the soil of the study area (PSREZ)

revealed significant relationships among various PTEs, providing insights into their sources, behavior, and interactions in the soil environment. Cu exhibits strong positive correlations with Pb ( $r=0.90$ ), V ( $r=0.84$ ), Cr ( $r=0.88$ ), and Fe ( $r=0.77$ ). Pb shows even stronger correlations with V ( $r=0.94$ ) and Cr ( $r=0.89$ ), further supporting the likelihood of co-occurrence or similar environmental pathways. V and Cr have an exceptionally strong correlation ( $r=0.94$ ), as do V and Fe ( $r=0.95$ ), indicating common origins such as weathering of parent rocks or industrial emissions. Zn displays moderate correlations with Cu ( $r=0.64$ ) and Cd ( $r=0.51$ ), suggesting some degree of co-occurrence or shared environmental influences. Mn and P showed moderate to strong positive correlations ( $r=0.69$ ), likely due to their association with organic matter or involvement in similar biogeochemical cycles [34] (Fig. 5).

Hg shows weaker correlations with most elements, with the strongest relationship observed with Cu ( $r=0.64$ ). This may indicate localized contamination sources or unique geochemical behavior. Co exhibits negative correlations with most elements, particularly with Cu ( $r=-0.59$ ) and Pb ( $r=-0.50$ ). This inverse relationship may result from competitive binding interactions or differing geochemical origins. Overall, the strong correlations between Cu, Pb, V, and Cr suggest a common source, for example, the weathering of the parent rocks. These elements also exhibit similar mobility patterns in the soil environment [34]. The inverse relationship observed between Co and other metals underscores the presence of competitive interactions or variations in geochemical processes, such as selective adsorption or leaching. Soil properties, including pH levels, organic matter content, and cation exchange capacity are critical factors influencing the retention and bioavailability of metals. For

**Table 4** Potential single and multi-elements pollution index in soil samples from the study area at two depth intervals (0–5 cm and 5–20 cm)

	Element	0–5 cm				5–20 cm			
		Mean	Min–Max	Med	Stdev	Mean	Min–Max	Med	Stdev
Single elements pollution indices	Cu	1.06	0.5–2.4	0.9	0.46	0.38	0.2–0.7	0.38	0.1
	Cd	1.42	0.6–2.7	1.12	0.6	1.4	0.8–1.6	1.4	0.213
	Co	0.6	0.5–0.7	0.6	0.07	0.8	0.6–1	0.8	0.09
	Pb	2.9	1.6–8.8	2.76	1.61	1.4	0.9–2.1	1.39	0.29
	Zn	0.27	0.09–0.6	0.195	0.162	0.13	0.06–0.8	0.105	0.147
	Cr	0.4	0.2–0.9	0.44	0.18	0.21	0.11–0.3	0.18	0.07
	Ni	8.28	1–14.8	8.5	3.92	4.03	1.09–9.8	2.77	2.55
	Mn	0.2	0.02–0.6	0.12	0.19	0.1	0.018–0.3	0.09	0.07
	Fe	0.26	0.1–0.6	0.26	0.1	0.1	0.07–0.2	0.14	0.05
Hg	1.4	0.3–6.6	0.8	1.5	0.52	0.1–1.6	0.4	0.39	
Multi-elements pollution index	RI=Σ SEPI	17	6.6–32.3	17.4	6.8	9.3	5.3–15.9	8.1	3.1

example, elevated organic matter content in soil can diminish the mobility and bioavailability of metals [34–37].

The weak positive correlations between  $^{137}\text{Cs}$  and elements like Cu, Pb, V, Cr, Ni, Mn, and Hg suggest that they have different sources of provenance. The negligible correlation with Cd and the weak negative correlation with Co highlight that  $^{137}\text{Cs}$  behave independently of these elements, which could be due to differences in their sources, chemical properties, or environmental mobility [38]. The matrix highlights the complexity of the interactions between elements and radionuclides in environmental systems, which is critical for understanding contamination and remediation strategies.

### Assessment of $^{137}\text{Cs}$

According to previously performed studies in Polesie State Radiation and Ecological Reserve, the primary contamination with  $^{137}\text{Cs}$  was formed on the soil surface and above-ground parts of plants. A significant part of the radionuclide activity from the plant surface soon also ended up on the soil surface. Under the influence of atmospheric precipitation and biological processes, a slow migration of contamination into the soil occurred. However, even today, more than 50% of the  $^{137}\text{Cs}$  remain predominantly in the upper 10 cm soil layer, and in most cases in the upper 5 cm layer. The rate of vertical migration of the radionuclide is 0.22–0.75 cm/year depending on the soil type [39]. In the forest ecosystems, the litter plays an important role in the redistribution of  $^{137}\text{Cs}$ . Its specific activity is significantly higher than that in the mineral horizons of the soil. Thus, in the pine plantations of the PSRER, the content of  $^{137}\text{Cs}$  in the litter reaches 138 KBq/kg, and in black alder forests—170 KBq/kg [40].

The present data of the study area (Table 5) reveal a distinct vertical distribution of  $^{137}\text{Cs}$ , with significantly higher

concentrations in the topsoil (0–5 cm) compared to the deeper layers (5–20 cm). Specifically, the  $^{137}\text{Cs}$  activity in the 0–5 cm samples ranged from 991.4 Bq/kg to 117,947 Bq/kg, with an average of 2,315 Bq/kg, indicating substantial surface contamination due to the direct deposition of radioactive fallout. In contrast, the 5–20 cm samples show a lower range of 183.2 Bq/kg to 40,710 Bq/kg, with an average of 5,148 Bq/kg, suggesting limited vertical migration of  $^{137}\text{Cs}$ . Figure 6 illustrates the spatial distribution of  $^{137}\text{Cs}$  in the soil across the study area, revealing that the highest activity concentrations are predominantly localized in the southeastern region. This observation is consistent with the findings reported in previous studies [20, 21].

The average activity in the upper layer was more than four times higher than that in the deeper layer, consistent with  $^{137}\text{Cs}$ 's behavior as a fallout radionuclide that binds strongly to surface soil particles [41]. However, the presence of  $^{137}\text{Cs}$  at greater depths indicates some degree of vertical migration, likely driven by soil disturbance, leaching, biological activity, or factors such as soil type, rainfall, and agricultural practices [41–43].

The elevated  $^{137}\text{Cs}$  levels in the Polesie State Reserve starkly contrast with the global background levels, which typically remain below 10 Bq/kg in uncontaminated areas [43]. This disparity underscores the persistent impact of the Chernobyl-derived radioactive contamination in the region. The upper soil activity concentrations in the reserve are comparable to those observed in other heavily contaminated areas, such as the Red Forest within the Chernobyl Exclusion Zone, where  $^{137}\text{Cs}$  levels can exceed 100,000 Bq/kg in localized hotspots [44]. Similarly, other forests in Belarus exhibit  $^{137}\text{Cs}$  activity concentrations ranging from 1000 to 50,000 Bq/kg, influenced by proximity to the Chernobyl reactor and variations in soil type and vegetation cover [45].

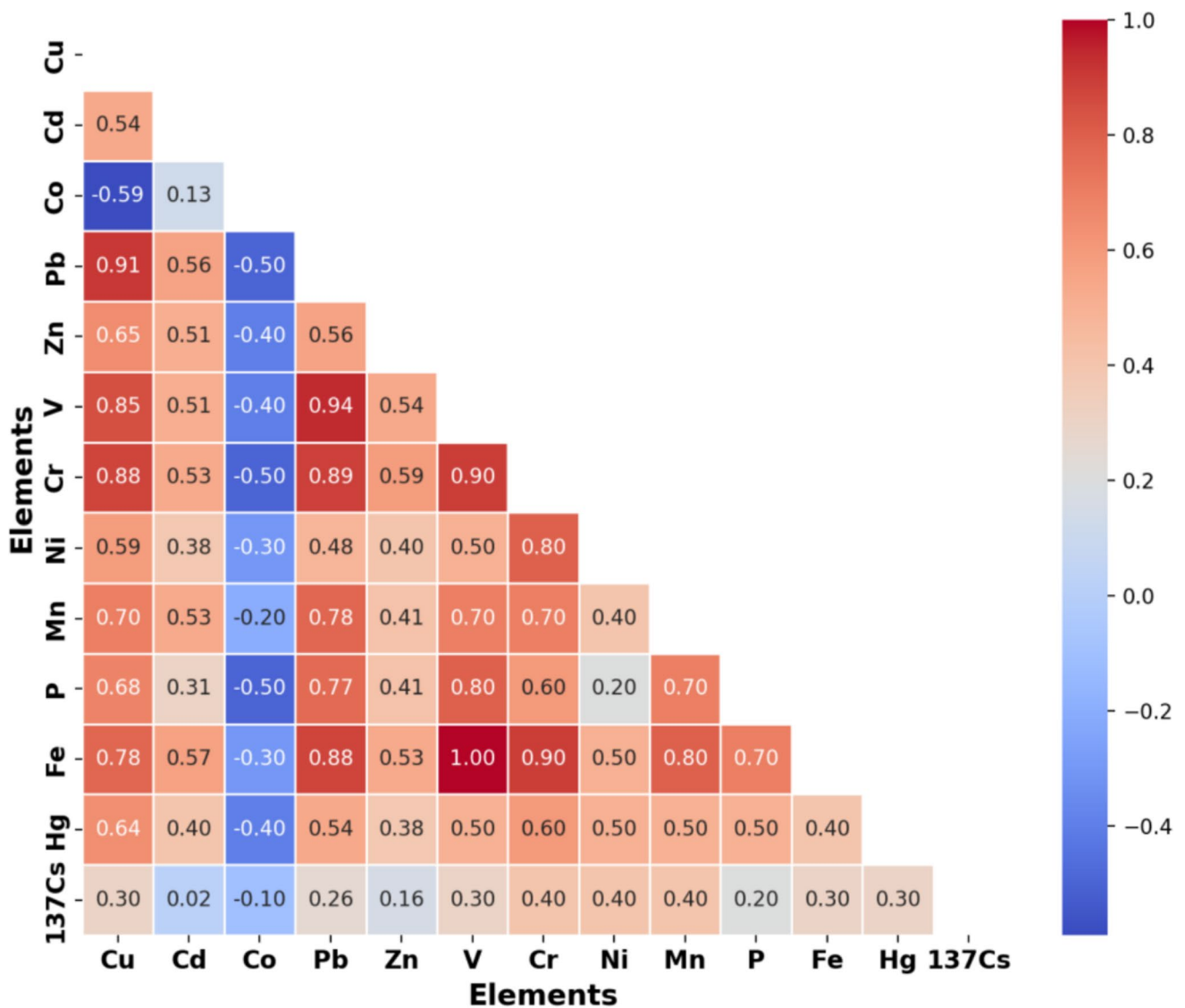
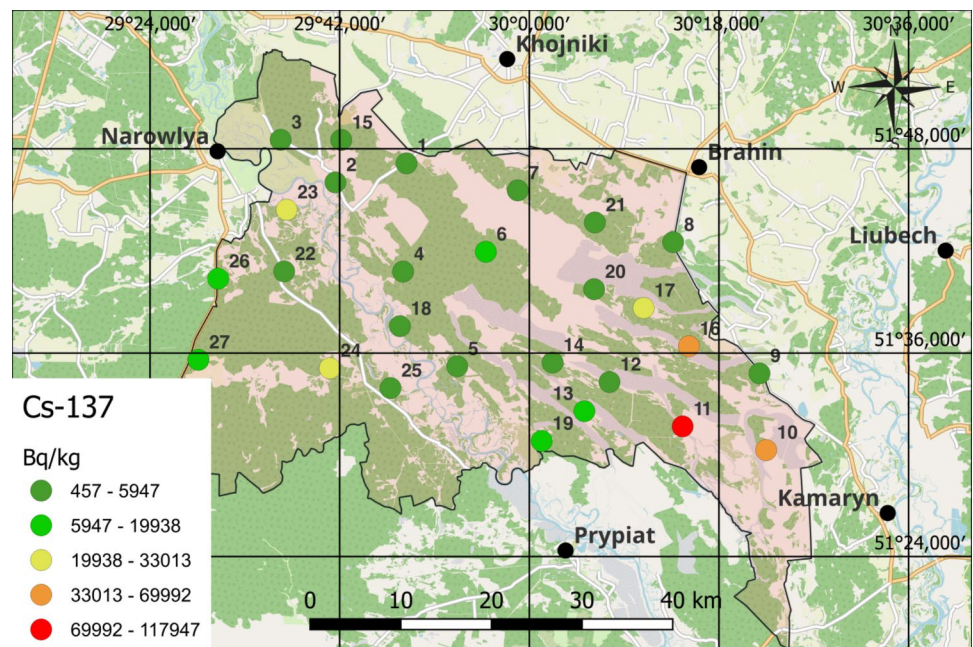


**Fig. 5** Pearson correlation coefficient of the studied potentially toxic elements and <sup>137</sup>Cs. In the Radiation and Ecological Reserve of Polesie State, Belarus

**Table 5** Comparison of <sup>137</sup>Cs activity concentrations in soil samples from the Polesie State Radiation and Ecological Reserve and other regions

Region	Soil depth (cm)	<sup>137</sup> Cs activity (Bq/kg)	Source
Polesie State Radiation and Ecological Reserve, Belarus	0–5	991–117,947 (Avg: 23 149)	Present work
Polesie State Radiation and Ecological Reserve, Belarus	5–20	183–40,710 (Avg: 5 148)	Present work
Red Forest, Chernobyl Exclusion Zone	0–5	Up to 100,000 (Hotspots)	[44]
Other forests in Belarus	0–20	1000–50,000	[45]
Ivankov District, Ukraine	0–20	6–390	[15]
Northern Ukraine	0–20	Up to 1,480,000 (kBq/m <sup>2</sup> )	[15]
Chernobyl exclusion Zone, Russia	0–30	Up to 250,000	[43, 46]
Global Background Levels	0–20	< 10	[43]
Designated area of 1 km <sup>2</sup> Northern Greece in 1987	0–5	311	[47]
Designated area of 1 km <sup>2</sup> Northern Greece in 2023	0–5	39	[47]
Designated area of 1 km <sup>2</sup> Northern Greece in 1987	5–20	25	[47]
Designated area of 1 km <sup>2</sup> Northern Greece in 2023	5–20	27	[47]

**Fig. 6** Map showing the distribution pattern of  $^{137}\text{Cs}$  in the soil of the study area



Compared to other regions affected by the Chernobyl disaster, a heterogeneous contamination landscape emerges. In Ukraine, soil samples from the Ivankov district show  $^{137}\text{Cs}$  activity concentrations ranging from 6 to 390 Bq/kg, while areas in northern Ukraine report contamination levels exceeding 1480 kBq/m<sup>2</sup> in the most affected regions [15]. In Russia, particularly near the Chernobyl Exclusion Zone, soil contamination patterns exhibit similar irregularities, with some areas reporting concentrations exceeding 250 kBq/kg within 30 km of the Chernobyl Nuclear Power Plant [43, 46]. Contaminated agricultural soils across Ukraine cover approximately 8.4 million hectares, highlighting the extensive impact of the disaster [15] Table 5. Based on the long-term monitoring study by [47], the activity concentration of  $^{137}\text{Cs}$  in soil in the designated area of ~1000 m<sup>2</sup> within the University farm of Aristotle University of Thessaloniki in Northern Greece was utilized by the Nuclear Technology Laboratory as a test ground for radioecological measurements exhibited pronounced redistribution between 1987 and 2023. In the surface layer (0–5 cm), concentrations decreased dramatically from 311 Bq/kg in 1987 to 39 Bq/kg in 2023, reflecting significant vertical migration of radionuclides over the 36-year period. Conversely, in the subsurface layer (5–20 cm), concentrations remained relatively stable, increasing slightly from 25 Bq/kg to 27 Bq/kg during the same interval [47].

The elevated concentration of  $^{137}\text{Cs}$  in the upper layers of forest soils in Belarus are attributed to a combination of inter-related factors linked to the aftermath of the Chernobyl accident. These factors include atmospheric deposition, soil dynamics, biological activity, soil disturbance, and soil chemical properties. Atmospheric deposition played a critical role

in the initial introduction of  $^{137}\text{Cs}$  into the ecosystems, as the radionuclide was dispersed and subsequently deposited onto the soil surface. Soil dynamics, such as the movement of water and organic matter, further influence the vertical distribution of  $^{137}\text{Cs}$ , often resulting in its retention in the topsoil. Biological activity, including the uptake and cycling of  $^{137}\text{Cs}$  by plants and microorganisms, contributes to its concentration in the upper soil layers. Additionally, soil disturbance, whether through natural processes or human activities, can redistribute  $^{137}\text{Cs}$  within the soil profile. Finally, the chemical properties of the soil, particularly the presence of clay minerals and organic matter, enhance the adsorption and immobilization of  $^{137}\text{Cs}$ , preventing its migration to deeper layers [41, 45, 46]. Collectively, these factors explain the persistence and higher concentration of  $^{137}\text{Cs}$  in the upper soil layers of forest ecosystems in Belarus.

The findings from the Polesie State Radiation and Ecological Reserve emphasize the enduring environmental legacy of the Chernobyl disaster. The high concentrations of  $^{137}\text{Cs}$ , particularly in the upper soil layers, reflect ongoing radiological challenges that necessitate further research and long-term monitoring. Such efforts are crucial for evaluating the ecological recovery in contaminated regions and developing effective remediation strategies. Additionally, raising public awareness and implementing regulatory measures are essential to minimize human exposure to residual radionuclides in the affected areas.

## Conclusions and recommendations

An analysis of PTEs and  $^{137}\text{Cs}$  levels in the soils of the Polesie State Radiation and Ecological Reserve was conducted to evaluate the environmental risks. The findings, based on pollution load classifications and contamination degree indices, revealed that the majority of soils were uncontaminated in terms of PTEs. The consistently negative geo-accumulation index (Igeo) values across both soil depths (upper and lower layers) suggest that, although some PTEs are present, the area is not significantly affected by anthropogenic activities, particularly in the deeper soil layers. This indicates a relatively low immediate threat of industrial pollution in this region. However, the activity concentration of  $^{137}\text{Cs}$  was found to exceed the global average, reflecting the legacy of the Chernobyl disaster. The elevated levels of  $^{137}\text{Cs}$ , particularly in the localized hotspots, underscore the uneven distribution of this radionuclide in the environment. While the Polesie State Radiation and Ecological Reserve exhibits some of the highest  $^{137}\text{Cs}$  concentrations documented post-Chernobyl, neighboring regions such as Ukraine and Russia also display complex mosaics of contamination levels, shaped by their unique environmental contexts and historical exposure to radioactive fallout. The presence of  $^{137}\text{Cs}$  poses significant long-term ecological and health risks, necessitating continuous monitoring and targeted remediation strategies.

The radionuclide contamination and the presence of PTEs highlight the complex dynamics of environmental pollution in Belarus. Continued research is essential to better understand these interactions and to develop effective measures for mitigating the long-term impacts of  $^{137}\text{Cs}$  on human health and ecosystems. This study emphasizes the importance of addressing localized contamination hotspots and implementing region-specific strategies to manage environmental risks in the Polesie State Radiation and Ecological Reserve and beyond.

Given the concerning accumulation of high-specific-activity  $^{137}\text{Cs}$  within the study area, merely informing governmental bodies is insufficient. Sustained, targeted scientific investigation is essential to understand contamination dynamics and identify effective remediation pathways. The authors therefore recommend prioritizing long-term research—potentially leveraging AI-assisted radiation monitoring networks and community-led soil management programs to guide actionable strategies. Additionally, it is important to provide practical recommendations not only to policymakers but also to the broader scientific community and relevant stakeholders, thereby fostering collaborative solutions.

**Author contributions** N.Y.: samples collection, investigation, map preparation. M.M.G.: original draft preparation, visualization, resources, data curation. A.N.: conceptualization, samples collection, data validation, original draft preparation. E.V.M., D.V.S, O.A.S and G.A.L: samples collection, investigation. A.S. and E.S: samples collection: I.Z.: conceptualization, data validation, original draft preparation. All authors have read and agreed to the published version of the manuscript.

**Funding** No external funding was received for this study.

**Data availability** Not applicable.

## Declarations

**Conflict of interest** The authors declare that they have no conflict of interest.

**Ethical approval** Not applicable.

**Consent to participate** Not applicable.

**Consent for publication** Not applicable.

## References

1. El-Taher A, Zakaly HMH, Elsaman R (2018) Environmental implications and spatial distribution of natural radionuclides and heavy metals in sediments from four harbors in the Egyptian Red Sea coast. *Appl Radiat Isot* 131:13–22. <https://doi.org/10.1016/j.apradiso.2017.11.012>
2. Bychinsky VA, Charykova MV, Omara R (2021) Geochemical modeling of soil and technogenic sediment interactions with natural waters using SELECTOR software (Chaabet-el-Hamra mine, Algeria). *Geochemistry* 81:125799. <https://doi.org/10.1016/j.chemer.2021.125799>
3. Ali MM, Rahman S, Islam MS, Rakib MRJ, Hossen S, Rahman MZ, Kormoker T, Idris AM, Phoungthong K (2022) Distribution of heavy metals in water and sediment of an urban river in a developing country: a probabilistic risk assessment. *Int J Sediment Res* 37(2):173–187
4. Khomich VS, Parfenov VV, Savchenko SV (2022) Trends of soil contamination with heavy metals and oil products in the cities of Belarus. *Nat Manag* 2:112–121. <https://doi.org/10.1007/s10661-022-09999-2>
5. Akter S, Jolly YN, Kabir J, Mamun KM, Rahman MO, Hasan M et al (2023) Heavy metal contamination of surface soils by anthropogenic activities: concomitant ecological and health risk assessment. *Int J Environ Anal Chem.* <https://doi.org/10.1080/03067319.2023.2171234>
6. Ene A, Sloță F, Frontasyeva MV, Duliu OG, Sion A, Gosav S et al (2024) Multi-element characterization of soils in the vicinity of siderurgical industries: levels, depth migration, and toxic risk. *Minerals* 14(6):559. <https://doi.org/10.3390/min14060559>
7. Mahmoud MG, Salem SG, Lotfy IM, Dawoud MM, Abu-Elhasan M, Elithy MA (2024) Ecological risk assessment of heavy metal pollution in the recent sediments of Qaroun Lake, Fayoum, Egypt. *Egypt J Chem* 67(3):487–501. <https://doi.org/10.21608/ejchem.2024.123456>
8. Alghanimi SMK, Chamani A, Almusawi AN, Tavabe KR (2024) Potentially toxic elements risk assessment and source identification of an at-risk international wetland in SW Iran. *Wetlands* 44(1):63. <https://doi.org/10.1007/s13157-024-01812-5>

9. Nguyen MD, Vo TQT, Tran QT, Tran TA, Tuong TTH, Nguyen THL et al (2025) Assessment of potentially toxic and rare earth elements in the surface soils of Dong Nai. Vietnam Environ Geochem Health 47(1):1–21. <https://doi.org/10.1007/s10653-024-01912-5>
10. Rinklebe J, Antoniadis V, Shaheen SM, Rosche O, Altermann M (2019) Health risk assessment of potentially toxic elements in soils along the Central Elbe River, Germany. Environ Int 126:76–88. <https://doi.org/10.1016/j.envint.2019.02.011>
11. Jahandari A, Abbasnejad A, Jamasb R (2020) Concentration, likely sources, and ecological risk assessment of potentially toxic elements in urban soils of Shiraz City, SW Iran. Arab J Geosci 5:35. <https://doi.org/10.1007/s12517-020-05345-3>
12. Gad A, Saleh A, Farhat HI, Dawood YH, Abd El Bakey SM (2022) Spatial distribution, contamination levels, and health risk assessment of potentially toxic elements in household dust in Cairo City. Egypt Toxics 10(8):466. <https://doi.org/10.3390/toxics10080466>
13. Panova EG, Bakhmatova KA, Matinian NN, Oleynikova GA (2020) Determination of the water-soluble fraction in soils. Processes and phenomena on the boundary between biogenic and abiogenic nature. Springer, New York, pp 155–178. [https://doi.org/10.1007/978-3-030-21614-6\\_10](https://doi.org/10.1007/978-3-030-21614-6_10)
14. Gunko NV, Ivanova OM, Korotkova NV, Buderatska VB, Boiko ZN, Masiuk SV et al (2022) Radioactively contaminated territories of the Chernihivska Oblast of Ukraine: the radiation-ecological and medical-demographic past and present. Probl Radiac Med Radiobiol 27:167–187. <https://doi.org/10.33145/2304-8336-2022-27-167-187>
15. IAEA (2006) Environmental consequences of the Chernobyl accident and their remediation: twenty years of experience. Report of the Chernobyl Forum Expert Group ‘Environment’. STI/PUB/1239, International Atomic Energy Agency, Vienna
16. Chernysh Y, Chubur V, Ablicieva I, Skvortsova P, Yakhnenko O, Skydanenko M et al (2024) Soil contamination by heavy metals and radionuclides and related bioremediation techniques: a review. Soil Syst 8(2):36. <https://doi.org/10.3390/soilsystems8020036>
17. Deryabina TG, Kuchmel SV, Nagorskaya LL, Hinton TG, Beasley JC, Lerebours A et al (2015) Long-term census data reveal abundant wildlife populations at Chernobyl. Curr Biol 25(19):R824–R826. <https://doi.org/10.1016/j.cub.2015.08.017>
18. Ministry of Natural Resources and Environmental Protection of the Republic of Belarus (2021) National report on the state of the environment in Belarus. <https://www.minpriroda.gov.by/en>
19. Kalinichenko SA, Nikitin AN, Shurankova OA (2022) Influence of environmental conditions on the biological availability and accumulation of <sup>137</sup>Cs by meadow grasses in the exclusion zone. Izv Gomel Gos Univ im F Skoriny 3(132):48–54
20. Nikitin AN, Shurankova OA, Mishchenko EV, Leferd GA, Sukhareva DV, Solonenko EV, Kalinichenko SA (2024) Features of <sup>137</sup>Cs accumulation in the stem wood and bark of pine and birch in the Belarusian sector of the Chernobyl exclusion zone. Botanika (Issledovaniya) 53:180–188
21. Kalinin M, Tsybul'skaya Y, Chubrik N (2010) Belarus has experience in the reduction of radionuclides and heavy metal content in plants following the Chernobyl disaster. In: Kulakow PA, Pidlisnyuk VV (eds) Application of phytotechnologies for cleanup of industrial, agricultural, and wastewater contamination. Springer, New York, pp 1–10. [https://doi.org/10.1007/978-90-481-3592-9\\_1](https://doi.org/10.1007/978-90-481-3592-9_1)
22. GOST 17.4.4.02-84 (1984) Nature protection. Soils. Methods for sampling and preparation of soils for chemical, bacteriological, helminthological analysis. Standardinform, Moscow
23. Zinicovscaia I, Hramco C, Chaligava O, Yushin N, Grozdov D, Vergel K, Duca G (2021) Accumulation of potentially toxic elements in mosses collected in the Republic of Moldova. Plants 10(3):471. <https://doi.org/10.3390/plants10030471>
24. Zinicovscaia I, Chaligava O, Grozdov D, Noskov M, Nosov D, Maksimova B, Dyakova A, Apanasevich P, Dmitrieva E (2024) Determination of the level of natural radionuclides and <sup>137</sup>Cs in soil samples in the Kemerovo region, Russia: assessment of the health risk. J Radioanal Nucl Chem. <https://doi.org/10.1007/s10967-024-09412-5>
25. Muller G (1969) Index of geoaccumulation in sediments of the Rhine River. GeoJournal 2(2):108–118. <https://doi.org/10.1007/BF00206486>
26. Fernández JA, Carballeira A (2001) Evaluation of contamination, by different elements, in terrestrial mosses. Arch Environ Contam Toxicol 40(4):461–468. <https://doi.org/10.1007/s002440010203>
27. Vergel K, Zinicovscaia I, Yushin N, Frontasyeva MV (2019) Heavy metal atmospheric deposition study in the Moscow region. Russia Bull Environ Contam Toxicol 103(3):435–440. <https://doi.org/10.1007/s00128-019-02675-1>
28. Abdo SY, Zinicovscaia I, Yushin N, Chaligava O (2025) Using scleractinian corals as monitors of essential and potentially toxic elements pollution in the southern Red Sea, Yemen Republic. Cont Shelf Res 285:105390. <https://doi.org/10.1016/j.csr.2024.105390>
29. Poznyak SS (2011) Concentration of heavy metals (Pb, Ni, Zn, Cu, Mn, Zr, Cr, Co and Sn) in soils of the Central area of Belarus. Scientific journal of NRU ITMO. Econ Environ Manag Ser 1:250–261 ((In Russian))
30. Nguyen TBM, Trinh TMM, Zinicovscaia I, Le HK, Vergel K, Phan LT, Ha LA, Nguyen TTH, Cao VH (2024) Evaluation of soil contamination and health risks associated with consumption of *Brassica perviridis* grown on various soils collected in Northern Vietnam. J Radioanal Nucl Chem. <https://doi.org/10.1007/s10967-024-09783-1>
31. Hakanson L (1980) An ecological risk index for aquatic pollution control. A sedimentological approach. Water Res 14(8):975–1001. [https://doi.org/10.1016/0043-1354\(80\)90143-8](https://doi.org/10.1016/0043-1354(80)90143-8)
32. Tomlinson DL, Wilson JG, Harris CR, Jeffrey DW (1980) Problems in the assessment of heavy-metal levels in estuaries and the formation of a pollution index. Helgol Meeresunters 33(1):566–575. <https://doi.org/10.1007/BF02414780>
33. Buat-Menard P, Chesselet R (1979) Variable influence of the atmospheric flux on the trace metal chemistry of the oceanic suspended matter. Earth Planet Sci Lett 42(3):399–411. [https://doi.org/10.1016/0012-821X\(79\)90049-9](https://doi.org/10.1016/0012-821X(79)90049-9)
34. Wang J, Liu R, Zhang P, Yu W, Shen Z, Feng C (2015) Spatial variation, environmental assessment, and source identification of heavy metals in sediments of the Yangtze River Estuary. Mar Pollut Bull 98(1):244–251. <https://doi.org/10.1016/j.marpolbul.2015.06.048>
35. Wu Q, Leung JYS, Geng X, Chen S, Huang X, Li H, Huang Z, Zhu L, Chen J, Lu Y (2014) Heavy metal contamination of soil and water in the vicinity of an abandoned e-waste recycling site: implications for dissemination of heavy metals. Environ Sci Technol 48(13):7035–7043. <https://doi.org/10.1021/es501257v>
36. Mehr MR, Keshavarzi B, Moore F, Sharifi R, Lahijanzadeh A, Kermani M (2017) Distribution, source identification and health risk assessment of soil heavy metals in urban areas of Isfahan province, Iran. J Afr Earth Sci 132:16–26. <https://doi.org/10.1016/j.jafrearsci.2017.04.026>
37. Yushin N, Jakhu R, Chaligava O, Grozdov D, Zinicovscaia I (2024) Evaluation of the potentially toxic elements and radionuclides in the soil sample of Novaya Zemlya in the Arctic Circle. Environ Pollut 361:124871. <https://doi.org/10.1016/j.envpol.2024.124871>
38. Konoplev A, Golosov V, Laptev G, Nanba K, Onda Y, Takase T, Wakiyama Y, Yoshimura K (2016) Behavior of accidentally released radiocesium in soil–water environment: looking at

- Fukushima from a Chernobyl perspective. *J Environ Radioact* 151:568–578. <https://doi.org/10.1016/j.jenvrad.2015.06.019>
39. Goloveshkin VV, Nenashev RA, Belash VE, Balenok AA, Karandevich AA (2024) Influence of weather and climatic conditions on the parameters of radionuclide migration in soils of the Chernobyl exclusion zone. *Radiobiol Ecol Saf.* 56–60
  40. Shurankova OA, Nikitin AN, Cheshik IA, Mishchenko EV, Kalinichenko SA, Sukhareva DV, Zhukovskaya EV (2022) Stocks of  $^{137}\text{Cs}$  in the litter of pine and birch stands growing in the Polesye State Radiation–Ecological Reserve. *Probl For Sci For* 82:290–299
  41. Chaligava O, Grozdov D, Yushin N, Zinicovskaia I, Vergel K (2022) Distribution of natural and anthropogenic radionuclides in soil samples in the recreational zones of Moscow. *Water Air Soil Pollut* 233(1):448. <https://doi.org/10.1007/s11270-022-05888-1>
  42. Zhu YG, Shaw G (2000) Soil contamination with radionuclides and potential remediation. *Chemosphere* 41(1):121–128. [https://doi.org/10.1016/S0045-6535\(99\)00398-7](https://doi.org/10.1016/S0045-6535(99)00398-7)
  43. UNSCEAR (2000) Exposures from natural radiation sources. United Nations Scientific Committee on the Effects of Atomic Radiation, New York
  44. Yoschenko VI, Kashparov VA, Protsak VP, Lundin SM, Levchuk SE, Kadygrib AM, Zvarich SI, Khomutinin YV, Maloshtan IM, Lanshin VP, Kovtun MV, Tschiersch J (2006) Resuspension and redistribution of radionuclides during grassland and forest fires in the Chernobyl exclusion zone: Part I. Fire experiments. *J Environ Radioact* 86(2):143–163. <https://doi.org/10.1016/j.jenvrad.2005.08.004>
  45. Fesenko SV, Prudnikov PV, Isamov NN, Emlyutina ES, Titov IE (2022) Dynamics of  $^{137}\text{Cs}$  concentration in fodder in the long-term after the Chernobyl accident. *Biol Bull* 49(12):2359–2368. <https://doi.org/10.1134/S106235902212006X>
  46. Kashparov VA, Lundin SM, Zvarich SI, Yoschenko VI, Levchuk SE, Khomutinin YV (2003) Soil contamination with  $^{137}\text{Cs}$  in the near zone of the Chernobyl accident. *J Environ Radioact* 64(1):5–19. [https://doi.org/10.1016/S0265-931X\(02\)00039-7](https://doi.org/10.1016/S0265-931X(02)00039-7)
  47. Kaissas I, Clouvas A, Postatzis M, Xanthos S, Omirou M (2023) Long-term study (1987–2023) on the distribution of  $^{137}\text{Cs}$  in soil following the Chernobyl nuclear accident: a comparison of temporal migration measurements and compartment model predictions. *Radiat Prot Dosimetry* 199(19):2366–2372

**Publisher's Note** Springer Nature remains neutral with regard to jurisdictional claims in published maps and institutional affiliations.

Springer Nature or its licensor (e.g. a society or other partner) holds exclusive rights to this article under a publishing agreement with the author(s) or other rightsholder(s); author self-archiving of the accepted manuscript version of this article is solely governed by the terms of such publishing agreement and applicable law.